A MICRO HYDROGEN GENERATOR WITH A MICROFLUIDIC SELF-REGULATING VALVE FOR SENSORS AND FUEL CELLS

*Vikhram V. Swaminathan, L. Zhu, B. Gurau, R.I. Masel and M.A. Shannon**
University of Illinois at Urbana-Champaign, USA
*Corresponding Author: mshannon@illinois.edu

ABSTRACT

We have developed a fully integrated micro power generator, based on a hydrogen fuel cell. Key to the power generator is an on-board hydrogen production with a passive microfluidic control valve that provides self-regulating operation. Critical integration issues are identified and regimes established for efficient power generation. Preliminary results demonstrate the ability of our device to operate smoothly, with quick – order seconds – response for fluctuating power demands. Energy densities in excess of 150 Whr/L and peak powers of 369.2 W/L are promising for packaging the integrated hydrogen fuel cell into Power MEMS.

INTRODUCTION

Miniaturization of fuel-cell based power systems have been spurred by recent advances in microsystems. Among these, wireless sensors and bio-MEMS, for example, operate predominantly in the sub-milliwatt regime, with peak power requirement of about one milliwatt, and have duty cycles ranging from a few hours up to several days. Such systems require efficient power sources that can last over such periods of operation, and also meet the peak power demands in short bursts.

Fuel cells offer the promise of providing simultaneously higher power and energy densities than state-of-the-art batteries. However fuel cells have been successfully miniaturized down only to the centimeter scale, and focused on 1-10 W power generation for handheld electronic systems [1-3]. Scaling down further poses several challenges including fuel storage, handling, and control. In this paper, we demonstrate a fully integrated, millimeter-scale H_2-PEMFC, with an on-board hydrogen generator that readily supplies fuel through hydrolysis, which is controlled by a passive microfluidic valve that regulates water supply to the microreactor based on power demand encountered by the fuel cell.

Hydrogen Generator

Hydrogen generation is accomplished through controlled hydrolysis of calcium hydride (CaH_2), where

$$CaH_2 + 2H_2O \rightarrow Ca(OH)_2 + 2H_2\uparrow. \quad (1)$$

Numerous metallic hydrides have been identified as potentially high capacity sources of hydrogen [4]. The kinetics are influenced by the water-vapor partial pressure; the extent of reaction completeness; volume expansion; and solubility and porosity of the reaction products [5]. CaH_2 has a relatively high reaction rate and a hydrogen yield up to 90% [6], due to the hygroscopic, porous nature of by-product $Ca(OH)_2$. Allowance is made for volume expansion of 50% in designing the 4.4 mL capacity hydrogen generator, with a side-by-side hydride chamber and water reservoir configuration.

Fuel Cell

Hydrogen from the on-board CaH_2 source is used to run a miniaturized PEMFC. The membrane electrode assembly (MEA) for the H_2-PEMFC is comprised of a Nafion® 112 proton exchange membrane, and platinum black in a nafion-based ink as the catalyst. The MEA thickness is determined by factors such as resistivity, mass transport of protons and crossover of hydrogen, and strength against hydrogen pressure. In recent work done by our group [7], an air breathing cathode MEA showed peak power density as high as 280 mW/cm^2, which supplies the high-power density needed at the millimeter scale.

MEMS Control Valve

A microfabricated silicon control layer provides a fluidic connection between the water and hydride chambers to transport water for the hydrolysis reaction. It consists of holes aligned with the chambers', connected by a hydrophilic microchannel (150 µm wide × 5 µm deep × 2.2 mm long), and employs passive surface tension based pumping [8], due to capillary action (figure 1). The capillary pressure for a channel of width w and height h is described by the Young-Laplace equation

$$\Delta P = \rho\left(\frac{1}{r_1} + \frac{1}{r_2}\right), \quad (2)$$

with

$$2r_1 \cos\theta = h, \quad (3)$$

and

$$2r_2 \cos\theta = w, \quad (4)$$

where r_1 and r_2 are the principal radii of curvature for the meniscus, θ, the equilibrium contact angle, ρ, the surface tension of water, and ΔP, the pressure difference.

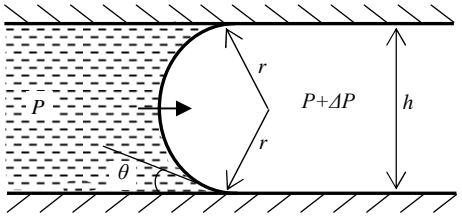

Figure 1: Surface tension pumping in a microchannel

A polyimide (PI) membrane bonded to the bottom of the control layer completes the channel geometry and forms a circular diaphragm valve below the water reservoir. A Cr/Au spot in the centre of the diaphragm provides water/hydrogen tight seal during valve closure. On the hydride side, a 300 µm hole creates a path for hydrogen to reach the MEA. A hydrophobic membrane, permitting water-vapor diffusion only, acts as a barrier to prevent liquid water from directly reacting with the CaH_2.

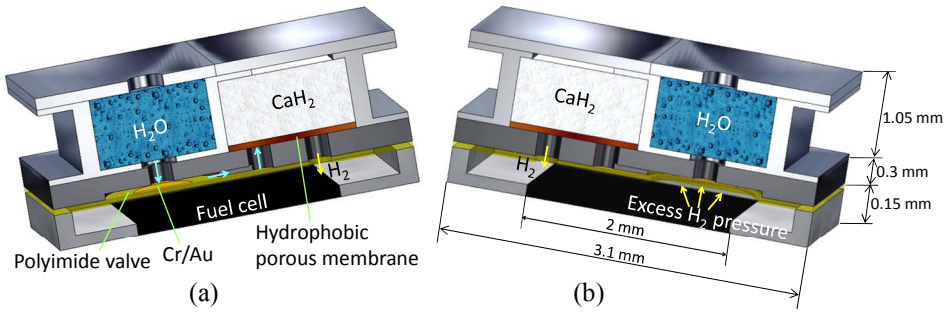

Figure 2: (a) Schematic of the integrated micro power generator, with a passive control valve, and (b) depicting the self-regulating action of the valve.

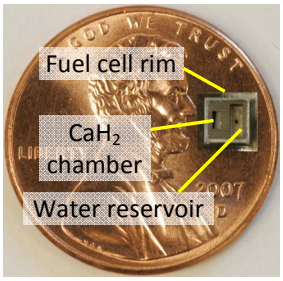

Figure 3: Photograph of the integrated device

The diameter and thickness of the diaphragm are estimated from plate theory with empirical modification [9], such that the pressure difference is

$$\Delta P = \frac{8}{3}\frac{Et}{a^4\left(1-\nu^2\right)}w_0^3 + 4\frac{\sigma_0 t}{a^2}w_0\,, \qquad (5)$$

where $w(r)$ is the analytical shape of the membrane, w_0, the maximum centre deflection, t, the thickness, a, the radius, σ_0, the uniform residual stress, and E and ν, the Young's modulus and Poisson's ratio for PI, respectively. For a 1 mm diameter and 2 µm thick membrane, the theoretical closing pressure is 3.7 KPa, which is significantly lower than the capillary pressure of 24 KPa, cf. equations (2-4). Thus, the valve responds and closes first to prevent hydrogen from breaching into the microchannel and equalizing pressure [10]. A distinct advantage of the control layer placement exposing water-laden PI-Si microchannel to the MEA is maintaining humidity around the anode to prevent Nafion® dry out.

Figure 2 depicts a schematic of the integrated device, with the operation of the microfluidic control valve, and a photo is shown is figure 3 for size comparison. The overall volume of the millimeter-scale device is 12.7 µL.

Device operation

During power generation, water flows into the microchannel, vapor diffuses through the hydrophobic porous membrane, and reacts with CaH_2 to rapidly release hydrogen that is consumed at the anode. When the electrical load drops, hydrogen accumulates in the space between the MEA and the control layer, causing a pressure differential across the diaphragm. The valve responds to cut-off water needed for the hydrolysis, and hydrogen production stops, preventing any further rise in pressure, which is insufficient to displace water in the microchannel, thus sending the device into a suspended state. Conversely, when power demand increases, hydrogen is consumed, leading to a pressure drop. The valve opens fully, delivering more water to the hydride; the device now operates in a hydrogen limited regime, governed by water-vapor diffusion towards unreacted hydride. Thus, the microfluidic control layer acts as a simple regulator, switching operating regimes with varying demand, providing load control without using power itself.

FABRICATION

Figure 4 shows a fabrication sequence, broadly based on aspects specific to components described above.

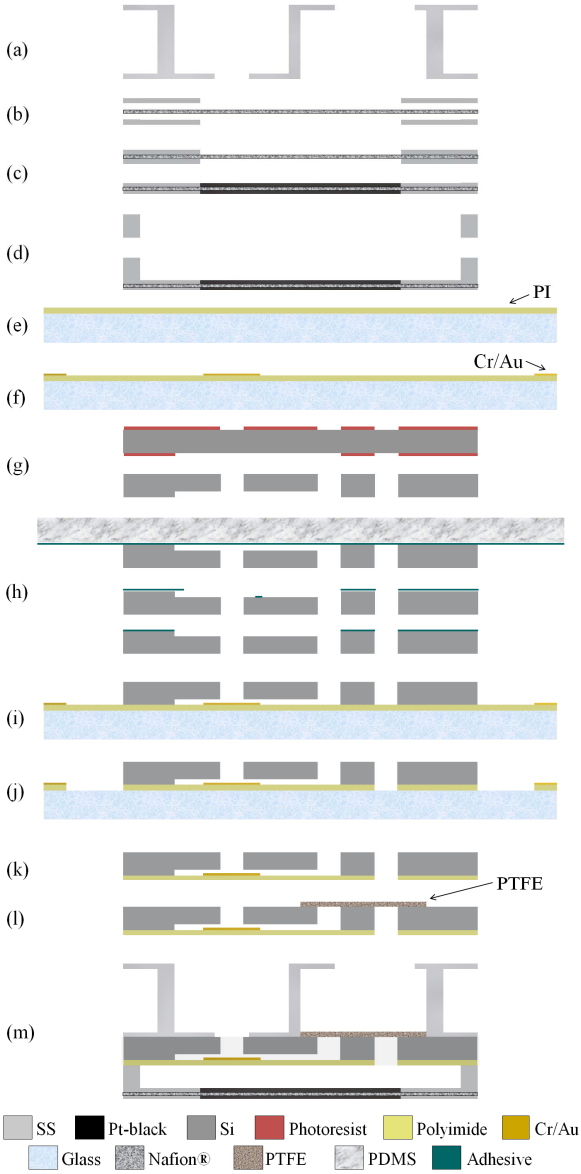

Figure 4: Fabrication flow sheet of the micro power generator.

The stainless steel (SS) hydrogen generator was electrical discharge machined, with rectangular water and hydride pockets. A 200-400 µm sized hole was provided at the bottom of the water chamber, whereas the hydride chamber bottom was left open with additional flange on the top to increase bonding surface. Material usage was economized and wall thickness reduced to 100 µm to increase volumetric energy density.

The MEA (figure 4(b)-(d)) was made by sandwiching Nafion® 112 between two 25 µm SS sheets, each having a laser cut window of 4 mm^2. Bonding was done by adhesive transfer of glue, thermally activated at 110°C, and cured at 140°C under hot pressing to form a strong, water-resistant bond [11]. Pt-black based catalyst ink was painted directly onto the PEM square windows on either side, adequately contacting the SS sheet, to create electrodes. A 50 µm thick SS spacer was bonded around the MEA using 3-M 2216™ two-part epoxy resin.

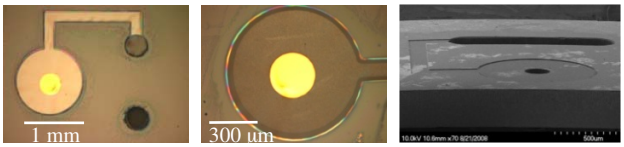

(a) (b) (c)

Figure 5: Images of the control layer. (a) PI membrane, microchannel and holes, (b) Cr/Au covering the water hole, and (c) SEM of Si control layer with a slot opening.

The control layer, shown in figure 5, was made using conventional microfabrication. The PI membrane was prepared through a spin-cure-release procedure (figure 4(e), (f)). A 25 mm square coverglass was treated by buffered HF and SC1 cleaning (NH_4OH:H_2O_2:H_2O - 1:10:100 at 73°C for 30 min). HD Microsystems™ PI 2545 precursor was spun at 3000 rpm and baked on a hotplate at 90°C for 30 min. Imidization to 2.3 µm final thickness was achieved, by vacuum annealing in N_2, at 350°C for 3 hours. A 200 nm thick Au film on 5 nm Cr adhesion layer was sputtered onto the PI surface. Micromachined Si shadow masks were used with patterns of alignment marks and the 200/300 µm Cr/Au spot for covering the 100/200 µm water hole. The Si die was patterned using double sided photolithography and SF_6/C_4F_8 plasma etching in a PlasmaTherm™ ICP-DRIE (figure 4(g)). The bottom channel was etched 6.3 µm deep, and freshly masked by 100 nm sputtered Al, before etching through holes from the top. SC-1 cleaning was performed to make the channel walls hydrophilic ($\theta \leq 5°$) [12]. As shown in (figure 4(h)-(k)), the transfer bonding was done by a PDMS-Si contact printing process [11]. Using a shadow mask, adhesive in the channel was removed by isotropic O_2 plasma RIE. With precise alignment of the Cr/Au spot, Si was thermally bonded to PI at 140°C. PI covering the H_2 hole and around Si was etched away by O_2 plasma and shadow masking. The samples were released overnight in a DI water bath on a hotplate at 120°C. A 25 µm PTFE hydrophobic membrane was attached to cover the hydride holes, and finally, the three layers were stacked and bonded by epoxy resin (figure 4(l) & (m)). The device was loaded with powdered CaH_2 supplied by Aldrich Chemical Co. (St. Louis, MO) and capped with a SS cover using Loctite Super Glue™, in a Nitrogen Glovebox.

TESTS AND RESULTS

Three specimens of the fully integrated micro power generator were tested, using a SI 1287 Potentiostat (Solartron Analytical, Hampshire, UK), to obtain various performance metrics. At the start of each experiment, Millipore water was added to the water chamber using a syringe. The first device had a control layer with a slot, and was used to obtain I-V characteristics. It was subsequently tested in switching mode, using ten, 10 min square waves of 0.8/0.3 V. The other two were tested for operating lifetime and energy density: the device with a 400 µm water delivery hole at 0.6 V; and the third with a 500 µm hole at 0.9 V. Results are depicted in figures 6-8 and summarized in Table 1.

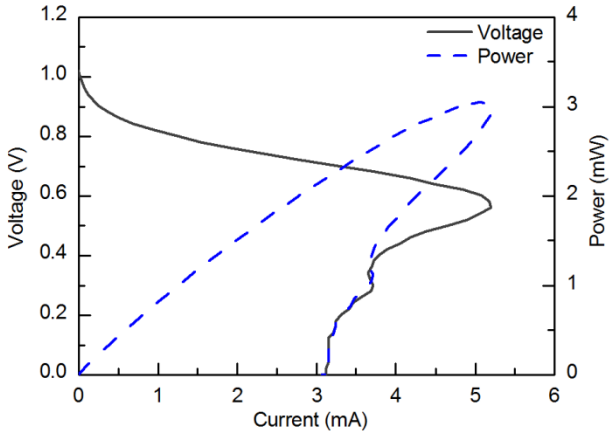

Figure 6: Polarization and theoretical power curve

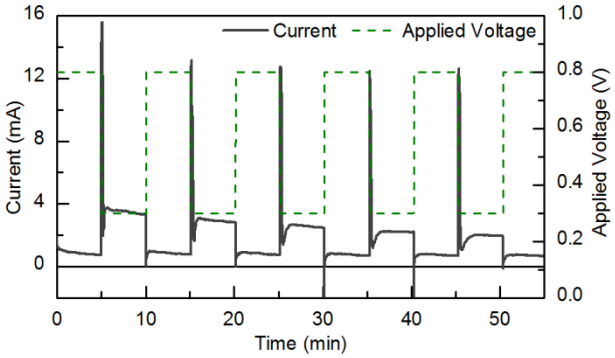

Figure 7: Square wave response between 0.8 and 0.3 V operating voltage; Peak Power density was 369.2 W/L

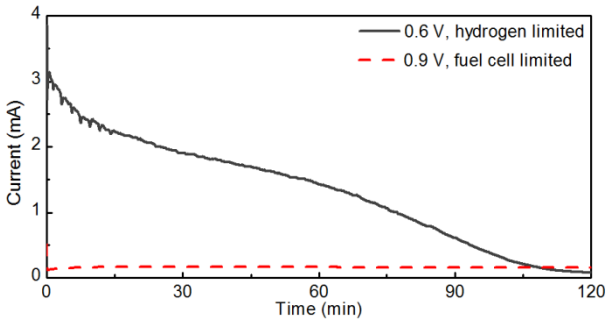

Figure 8: Chronoamperograms at two operating regimes

DISCUSSION

Numerous effects arise as a consequence of miniaturizing the H_2-PEMFC, evident from our results. The polarization and theoretical power curves suggest substantial drop in performance upon integration. The curves change direction when operated as high as 0.6 V, which indicates a H_2 mass transfer limit for the hydrogen generator. However, a high open circuit voltage of 1 V and the kinetic limit within 0.8 V imply the possibility of highly efficient power generation at sub-milliwatt capacities. The lifetime test on device 3 at 0.9 V generated

Table 1: Summary of test results for integrated devices

No.	Voltage (V)	Duration (hr)	Energy (Whr/L)	Peak Power (W/L)
1	0.8/0.3	1.67	83	369.2
2	0.6	2	152.1	159.4
3	0.9	10.5	86.75	31.86

a steady current during fuel cell limited operation. Running the device below 0.6 V for increased power is possible, but at reduced efficiency due to mass transport limitations.

Figure 7 depicts switching between high and low loads. The response shows the control of the water transport through the microfluidic channels to the hydride and the subsequent transport of the hydrogen to the MEA. The figure also shows the maximum power capacity of the device over a long period of dynamic operation. During the 5 min dwell times, we observed smooth current generation that gradually decreased over time due to a decrease in a mass transfer of H_2O into the generator and the H_2 gas out through the product hydrate. The nearly flat slope at 0.8 V shows fuel cell operating near the kinetic limit; but a small gradient arises from slowing of the hydrolysis reaction due to the increase in diffusion length for the water vapor to reach the hydride. The sharp peaks observed to be consistently in excess of 300 W/L while switching from 0.8 V to 0.3 V show that excess H_2 generation was sustained for long periods, and that the rapid change in load consumed the H_2 to meet demand. The drop to a lower value occurred as a consequence of a fully mass transport limited operation. However, current soon rose to levels predicted by the I-V curve, indicating the passive surface tension pumping of water in the microchannel to meet the H_2 demand. Similarly, the immediate drop upon switching back to a higher voltage, and settling into a steady operation with almost constant current, was made possible by successful closure of the valve, with its consequent increase in H_2 pressure.

The water-vapor diffusion limited H_2 generation theory was justified by a continuous, gradually decreasing current at 0.6 V operation. Figures 7 and 8 validate our approach and establish its versatility—the ability to generate power efficiently across different regimes, and respond to a dynamically varying demand. The energy density of the order of 150 Whr/L is on par with contemporary technologies, but high power capacity (369.2 W/L) and dynamic performance provide both high energy and power densities needed for many microsystems.

CONCLUSION

We have successfully demonstrated the concept of a self-regulating micro power generator with the capacity to generate H_2 on-demand for a fuel cell, with the ability to operate for long periods across multiple regimes, along with short bursts of high power density. The microfluidic control valve is sensitive to dynamically changing power requirements, without consuming power for control.

ACKNOWLEDGEMENTS

This research is funded by the Defense Advanced Research Projects Agency (DARPA) under U.S. Air Force grant FA8650-04-1-7121. Any opinions, findings, and conclusions or recommendations expressed in this manuscript are those of the authors and do not necessarily reflect the views of the US Government. Micro-Nano-Mechanical Systems Laboratory in University of Illinois at Urbana-Champaign provided the cleanroom facilities.

REFERENCES

[1] G.K. Pitcher, G.J. Kavarnos, "A Test Assembly for Hydrogen Production by the Hydrolysis of Solid Lithium Hydride", *Int. J. Hydrogen Energy*, vol. 22, no. 6, pp. 575-579, 1997.

[2] P.P. Prosini, P. Gislon, "A hydrogen refill for cellular phone", *J. Power Sources*, vol. 161, pp. 290-293, 2006.

[3] A.V. Pattekar, M.V. Kothare, "A Microreactor for Hydrogen Production in Micro Fuel Cell Application", *J. Microelectromech. S.*, vol. 13, no. 1, pp. 7-18, 2004.

[4] R. Aeillo, M.A. Matthews, D.L. Reger, J.E. Collins, "Production of Hydrogen Gas from Novel Chemical Hydrides", *Int. J. Hydrogen Energy*, vol. 23, no. 12, pp. 1103-1108, 1998.

[5] V.C.Y. Kong, D.W. Kirk, F.R. Foulkes, J.T. Hinatsu, "Development of Hydrogen Storage for Fuel Cell Generators II: Utilization of Calcium Hydride and Lithium Hydride", *Int. J. Hydrogen Energy*, vol. 28, pp. 205-214, 2003.

[6] L. Zhu, D. Kim, H. S. Kim, R.I. Masel, M.A. Shannon, "Hydrogen Generation from Hydrides in Millimeter Scale Reactors for Micro Proton Exchange Membrane Fuel Cell Applications", *J. Power Sources*, 2008, in press.

[7] B. Gurau, L. Zhu, H.S. Kim, R.D. Morgan, V. Vilasur Swaminathan, M.A. Shannon, R.I. Masel, "Integrated Miniature Fuel Cell – Hydrogen Generator for Portable Power Generation", *Proc. ECS PRiME*, 2008.

[8] G.M. Walker, D.J. Beebe, "A Passive Pumping Method for Microfluidic Devices", *Lab Chip*, vol. 2, pp. 131-134, 2002.

[9] J.C. Selby, M.A. Shannon, K. Xu, J. Economy, "Sub-micrometer Solid-state Adhesive Bonding with Aromatic Thermosetting Copolyesters for the Assembly of Polyimide Membranes in Silicon-based Devices", *J. Micromech. Microeng.*, vol. 11, pp. 672-685, 2001.

[10] S. Moghaddam, E. Pengwang, R.I. Masel, M.A. Shannon, "A Self-regulating Hydrogen Generator for Micro Fuel Cells", *J. Power Sources*, vol. 185, pp. 445-450, 2008.

[11] B.R Flachsbart,., K. Wong, J. M. Iannacone, E. N. Abante, R. L. Vlach, P. A. Rauchfuss, P. W. Bohn, J. V. Sweedler, and M. A. Shannon, "Design and Fabrication of a Multilayered Polymer Microfluidic Chip with Nanofluidic Interconnects via Adhesive Contact Printing," *Lab-On-A-Chip,* vol. 6 no. 5, pp. 667-674, 2006.

[12] D-H Eom, G-B Lim, J-G Park, A.A. Busnaina, "Reaction of Ozone and H_2O_2 in NH_4OH Solutions and Their Reaction with Silicon Wafers" *Jpn. J. Appl. Phys.*, vol. 43, no. 6A, pp. 3335-3339, 2004.